

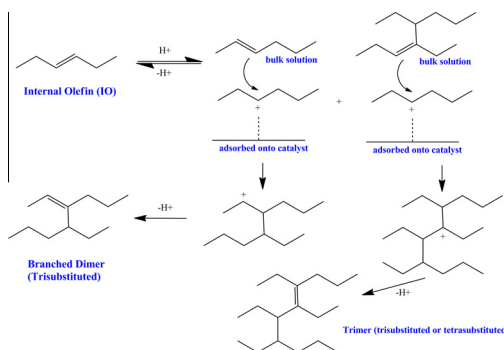


Contents

Dimerization of linear olefins on Amberlyst® 15: Effects of chain length and double-bond position

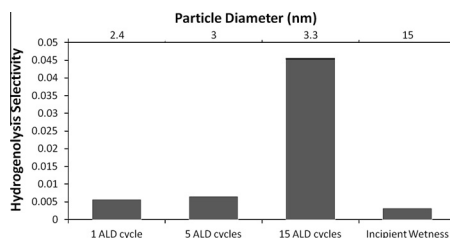
pp 1–8

Jeffrey C. Gee*, Shawn T. Williams

**Synthesis of supported Ni catalysts by atomic layer deposition**

pp 9–15

Troy D. Gould, Alia M. Lubers, Brian T. Neltner, Jacob V. Carrier, Alan W. Weimer, John L. Falconer, J. Will Medlin*

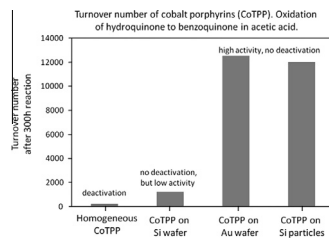


Supported Ni nanoparticles were synthesized via atomic layer deposition (ALD) with average particle sizes ranging from 2.4 to 3.3 nm and Ni weight loadings from 4.7 to 16.7%. This scalable gas-phase technique produced supported catalysts with enhanced propylene hydrogenolysis TOFs and selectivities. Enhanced catalytic activity was attributed to the step and kink defects induced from the small particle size. These defects, along with particle size were shown to vary with the number of ALD cycles.

Performance of a biomimetic oxidation catalyst immobilized on silica particles

pp 16–21

Kristofer Eriksson*, Emmanuelle Göthelid, Carla Puglia, Jan-E. Bäckvall, Sven Oscarsson*

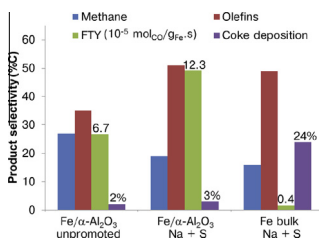


A biomimetic oxidation catalyst, cobalt porphyrin (CoTPP), was chemically grafted on silica particles and further used in oxidation of hydroquinone to benzoquinone. The activity was compared to earlier findings on gold and silicon wafers. It was found that the activity is the same as that on gold wafers, 10 times higher as that on silicon wafers, and it outperformed its homogenous counterpart by a factor of 100.

Effects of sodium and sulfur on catalytic performance of supported iron catalysts for the Fischer–Tropsch synthesis of lower olefins

pp 22–30

Hirsa M. Torres Galvis, Ard C.J. Koeken, Johannes H. Bitter, Thomas Davidian, Matthijs Ruitenbeek, A. Iulian Dugulan, Krijn P. de Jong*

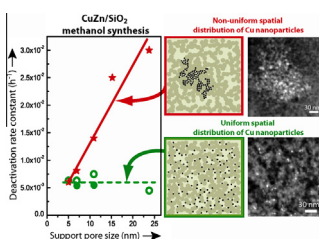


Catalysts promoted with low amounts of sodium and sulfur exhibited higher selectivity to lower olefins and lower methane production. Promoted bulk and α -Al₂O₃-supported catalysts showed similar selectivities; however, bulk catalysts displayed lower catalytic activity and extensive coke formation.

Interplay between pore size and nanoparticle spatial distribution: Consequences for the stability of CuZn/SiO₂ methanol synthesis catalysts

pp 31–40

Gonzalo Prieto*, Johannes D. Meeldijk, Krijn P. de Jong, Petra E. de Jongh*

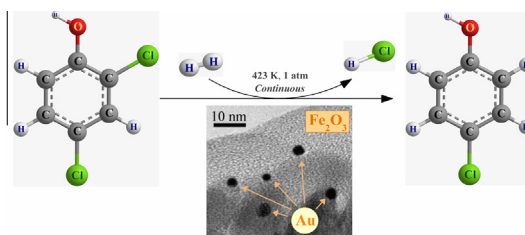


Support pore size and nanospacial distribution of the metal particles cooperatively determine catalyst stability.

Unique selectivity in the hydrodechlorination of 2,4-dichlorophenol over hematite-supported Au

pp 41–49

Santiago Gómez-Quero, Fernando Cárdenas-Lizana, Mark A. Keane*

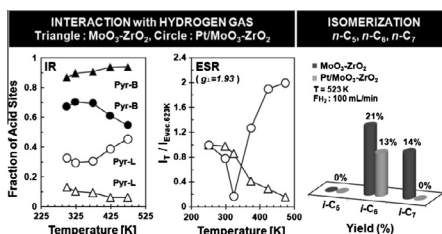


Nano-scale Au on Fe₂O₃ promotes selective hydrogenolysis of sterically constrained *ortho*-Cl from 2,4-dichlorophenol in continuous gas-phase operation.

C₅–C₇ linear alkane hydroisomerization over MoO₃–ZrO₂ and Pt/MoO₃–ZrO₂ catalysts

pp 50–59

S. Triwahyono*, A.A. Jalil, N.N. Ruslan, H.D. Setiabudi, N.H.N. Kamarudin



IR and ESR studies showed that the interaction of hydrogen with MoO₃–ZrO₂ formed protonic acid sites and electrons which led to change in the Mo oxidation state, whereas the interaction of hydrogen with Pt/MoO₃–ZrO₂ generated Lewis acid sites. The presence of Pt decreased the activity toward C₅–C₇ linear alkane hydroisomerization.

Download English Version:

<https://daneshyari.com/en/article/61249>

Download Persian Version:

<https://daneshyari.com/article/61249>

[Daneshyari.com](https://daneshyari.com)